



UNIVERSITÀ
DEGLI STUDI
FIRENZE

FLORE

Repository istituzionale dell'Università degli Studi di Firenze

Regularized Quadratic Penalty methods for Shape from Shading

Questa è la Versione finale referata (Post print/Accepted manuscript) della seguente pubblicazione:

Original Citation:

Regularized Quadratic Penalty methods for Shape from Shading / Stefania, Bellavia; Lapo Governi; Alessandra, Papini; Luca Puggelli. - In: MEDITERRANEAN JOURNAL OF MATHEMATICS. - ISSN 1660-5446. - STAMPA. - 14:(2017), pp. 0-0. [10.1007/s00009-017-0946-2]

Availability:

The webpage <https://hdl.handle.net/2158/1087697> of the repository was last updated on 2021-10-06T14:14:28Z

Published version:

DOI: 10.1007/s00009-017-0946-2

Terms of use:

Open Access

La pubblicazione è resa disponibile sotto le norme e i termini della licenza di deposito, secondo quanto stabilito dalla Policy per l'accesso aperto dell'Università degli Studi di Firenze (<https://www.sba.unifi.it/upload/policy-oa-2016-1.pdf>)

Publisher copyright claim:

Conformità alle politiche dell'editore / Compliance to publisher's policies

Questa versione della pubblicazione è conforme a quanto richiesto dalle politiche dell'editore in materia di copyright.

This version of the publication conforms to the publisher's copyright policies.

La data sopra indicata si riferisce all'ultimo aggiornamento della scheda del Repository FloRe - The above-mentioned date refers to the last update of the record in the Institutional Repository FloRe

(Article begins on next page)

Regularized quadratic penalty methods for shape from shading

Stefania Bellavia, Lapo Governi, Alessandra Papini and Luca Puggelli

Abstract. Shape from shading (SFS) denotes the problem of reconstructing a 3D surface, starting from a single shaded image which represents the surface itself. Minimization techniques are commonly used for solving the SFS problem, where the objective function is a weighted combination of the brightness error, plus one or more terms aiming to obtain a valid solution. We present a regularized quadratic penalty method where quadratic penalization is used to adaptively adjust the smoothing weights, and regularization improves the robustness and reliability of the procedure. A nonmonotone Barzilai-Borwein method is employed to efficiently solve the arising subproblems. Numerical results are provided showing the reliability of the proposed approach.

Keywords. Shape from shading, quadratic penalty methods, quadratic regularization, Barzilai-Borwein method.

AMS Subject Classification: 65C20; 65K05

1. Introduction

Shape from shading is a well known method for surface retrieval put forward in [15] which, as the name itself suggests, bases the reconstruction of the surface on the shading analysis of a single 2D image. Due to minimal available data, shape from shading is an intrinsically difficult and ill-posed problem, whose solution is based on the relationship linking surface normals, light direction and brightness at each point of the image. If the surface is Lambertian with constant albedo (i.e. the fraction of light that is reflected by the surface, with values between 0 and 1), the light source is sufficiently far from the scene as to consider the light beams as parallel, and the scene is not affected by distortions caused by optics, the following equation subsists

at any image point (x, y) :

$$L^T N(x, y) = \frac{1}{\rho} \mathcal{E}(x, y) \quad (1)$$

where: $L = [l_x, l_y, l_z]^T$ is the unit-vector opposed to light direction, $N(x, y) = [n_x(x, y), n_y(x, y), n_z(x, y)]^T$ is the unknown outward normal to the surface, ρ is the albedo, and $\mathcal{E}(x, y)$ the brightness, that is the normalized grey-level (between 0 and 1) of the given 2D image. This equation, named *irradiance equation*, has infinite valid solutions. In fact, (1) merely implies that the surface normal N lies on the lateral surface of the cone whose axis is parallel to L and whose semi-aperture θ depends on the brightness of the pixel itself as follows:

$$\theta(x, y) = \arccos(\mathcal{E}(x, y)/\rho).$$

Hence SFS is a challenging inverse problem which by adding suitable constraints aims to retrieve a specific surface that both satisfies (1) and best reproduces the expected one.

SFS has been extensively studied in literature, as it is shown by the long list of references in [30, 7, 27], but still of actual interest as it arises in a number of applications. The approaches proposed so far to solve the SFS problem can be divided into two main classes where research is still active [4, 7, 30]: methods based on resolution of PDE and variational methods.

The first approach attempts to directly solve the nonlinear partial differential equation obtained by rewriting equation (1) in terms of the unknown surface gradient. Let $z = u(x, y)$ denote the surface to be reconstructed, and

$$\nabla u(x, y) = \left[\frac{\partial u(x, y)}{\partial x}, \frac{\partial u(x, y)}{\partial y} \right]^T \equiv [p(x, y), q(x, y)]^T$$

its gradient. Recall that $N(x, y)$ can be expressed in terms of $[p(x, y), q(x, y)]$ as follows:

$$N(x, y) = \frac{[-p(x, y), -q(x, y), 1]^T}{\sqrt{1 + p(x, y)^2 + q(x, y)^2}}; \quad (2)$$

then using (2) in (1) we obtain the PDE

$$\frac{\mathcal{E}(x, y)}{\rho} \sqrt{1 + p(x, y)^2 + q(x, y)^2} = l_z - l_x p(x, y) - l_y q(x, y).$$

A number of papers appeared starting from works by Horn [15, 16]. Here we only mention [2, 10, 16, 20, 23, 25], referring to the two surveys [7, 30] for a comprehensive list.

Variational (or minimization) methods (see e.g. [4, 12, 14, 18, 19, 26, 29]) are instead based on the hypothesis that the expected surface minimizes an appositely designed functional. The main strength of this approach is its high robustness. In particular, minimization methods do not require perfectly shaded images, or exact settings (such as light direction), but allow in both cases some approximations. We refer to the review paper [7] for a thorough presentation of the two approaches; here we consider the variational one. The functional to be minimized is usually expressed in terms of surface normals

or surface gradients, since attempts to minimize directly with respect to the height may exhibit problems of convergence or slowness (see e.g. [7]). Then, a second step is needed to retrieve the height $u(x, y)$ corresponding to the computed surface normals or gradients. Though interesting by itself, this issue is out of the scope of this work, and we refer to [8, 12, 28] for a discussion on efficient methods performing this task. In our experiments we adopted the geometrical approach proposed in [28].

Several models have been proposed to solve the SFS problem via variational methods, for example:

$$\min_{p,q} \mathcal{B}(p, q) + \lambda_S \mathcal{S}(p, q), \quad (3)$$

$$\min_{p,q} \mathcal{B}(p, q) + \lambda_I \mathcal{I}(p, q), \quad (4)$$

or a combination of the previous two:

$$\min_{p,q} \mathcal{B}(p, q) + \lambda_S \mathcal{S}(p, q) + \lambda_I \mathcal{I}(p, q), \quad (5)$$

where

$$\mathcal{B}(p, q) = \int_{\Omega} [\mathcal{E}(x, y) - \rho L^T N(p(x, y), q(x, y))]^2 dx dy,$$

$$\mathcal{S}(p, q) = \int_{\Omega} [||\nabla p(x, y)||_2^2 + ||\nabla q(x, y)||_2^2] dx dy,$$

$$\mathcal{I}(p, q) = \int_{\Omega} \left(\frac{\partial p(x, y)}{\partial y} - \frac{\partial q(x, y)}{\partial x} \right)^2 dx dy.$$

$\mathcal{B}(p, q)$ is the *brightness* term, which forces the obtained normal map (or surface gradient) of the retrieved surface to satisfy equation (1) on the reconstruction domain Ω , that is to generate an image as close as possible to the input one, under the same lighting condition; $\mathcal{S}(p, q)$ is the *smoothness* term, that forces the retrieved surface slope to change gradually, and consequently to generate the smoothest surface possible; $\mathcal{I}(p, q)$ is the *integrability* term, used to generate integrable normal maps, i.e. normal maps relative to geometrically feasible surfaces. λ_S and λ_I are non-negative weights, called smoothness factor and integrability factor, respectively. Problems (3-5) are usually discretized and then solved by a number of algorithms, going from heuristic techniques to more complex gradient-based methods [7].

Each of the above models may render valid solutions provided λ_S and λ_I are suitably chosen. However, though crucial for the quality of the reconstructed surface, the choice of the parameters λ_S and λ_I has rarely been rigorously discussed, and is often left to heuristic/experimental considerations. Here, by using a penalty quadratic minimization approach [22], we devise a procedure for the solution of the (discretized) model (3) where an a-priori choice of the smoothing parameter λ_S is not needed anymore, since λ_S is adaptively adjusted.

Another known criticality of the variational approach is that the true solution may not exactly solve the model problem; indeed, the smoothness and integrability terms are in fact constraints to overcome the indefiniteness

of the irradiance equation by imposing additional regularity to the solution. As a consequence confirmed by experiments, the iterative methods used to solve an SFS minimization problem may in some cases walk away from the sought solution, even if this is given as initial guess (see e.g. [17]). In order to address this criticality of the variational approach, we propose a new regularized quadratic penalty method for shape from shading problems, where a suitable regularization term is added to the objective function at each step of the quadratic penalty approach. The convergence behaviour of the resulting approach is analyzed from a theoretical point of view. The procedure we present here is new in the context of SFS. We are only aware of the paper [21], where a continuation method is employed to adaptive choose the parameter λ_S . However in [21] minimization problems are solved directly with respect to surface height and the regularization term is not employed.

As a further contribution, we investigate on the application of the non-monotone Barzilai-Borwein method [24] for solving the minimization problems which arise in our regularized quadratic penalty procedure. Barzilai-Borwein is a globally convergent method of gradient-type endowed with a nonmonotone line-search technique. This choice is motivated by the following considerations. Gradient-type methods are particularly well-suited for this class of problems since functions and gradients evaluation can be performed at a low computational cost. Moreover, among other gradient-type algorithms, we focused on the Barzilai-Borwein one because of its faster practical convergence. This behaviour is due to the choice of the steplength, used in the line-search to update the iterate, which is somehow related to the spectrum of the Hessian [1, 3, 24]; indeed, the idea that such a steplength strategy speeds up the convergence of gradient methods has gained widespread acceptance in the last years [1, 5, 6].

Experiments performed so far, confirm the efficiency and reliability of the proposed procedure.

The paper is organized as follows. In Section 2 we introduce the discretized SFS problem. In Section 3 our regularized quadratic penalization approach is presented and analyzed. Algorithmic details are discussed in Section 4, while numerical results are reported in Section 5. Final remarks are given in Section 6.

2. Discretized SFS model

Let $E \in \mathbb{R}^{m \times n}$ denote the given input image discretized by an $m \times n$ grid of pixels, $N_{i,j} = [N_{x,ij}, N_{y,ij}, N_{z,ij}]^T$ the unit normal at pixel (i, j) , and $[p_{i,j}, q_{i,j}]$ the value of the vector $[p, q]$ at pixel (i, j) . Then the discretized brightness functional takes the form:

$$B(N) = \sum_{i=1}^m \sum_{j=1}^n [E_{i,j} - \rho L^T N_{i,j}]^2, \quad (6)$$

where

$$N = (N_{x,11}, N_{x,21}, \dots, N_{x,mn}, N_{y,11}, N_{y,21}, \dots, N_{y,mn}, \\ N_{z,11}, N_{z,21}, \dots, N_{z,mn})^T.$$

Further, using classical forward finite differences to replace gradients and partial derivatives of p and q , the smoothness and integrability terms are given by

$$S(\nu) = \sum_{i=1}^{m-1} \sum_{j=1}^{n-1} [(p_{i,j} - p_{i,j+1})^2 + (p_{i,j} - p_{i+1,j})^2 \\ + (q_{i,j} - q_{i,j+1})^2 + (q_{i,j} - q_{i+1,j})^2], \quad (7)$$

$$I(\nu) = \sum_{i=1}^{m-1} \sum_{j=1}^{n-1} (p_{i,j+1} - p_{i,j} - q_{i+1,j} + q_{i,j})^2, \quad (8)$$

with

$$\nu = (p_{11}, p_{21}, \dots, p_{n1}, p_{12}, \dots, p_{mn}, \\ q_{11}, q_{21}, \dots, q_{n1}, q_{12}, \dots, q_{mn})^T.$$

Recalling (2), we denote by $\mathcal{N} = \mathcal{N}(\nu)$ the nonlinear function of ν such that

$$\mathcal{N}_{i,j} = \mathcal{N}_{i,j}(\nu_{i,j}) = \frac{1}{\sqrt{1 + p_{i,j}^2 + q_{i,j}^2}} [-p_{i,j}, -q_{i,j}, 1]^T;$$

hence $B = B(\mathcal{N}(\nu))$ is a nonquadratic function of ν , which in the following will be simply denoted by $B(\nu)$.

In practice, the size of the unknown vector ν is reduced by removing background pixels from the discretized reconstruction domain, Ω_D . To this aim we used the interactive procedure proposed in [13], which allows to impose a set of suitable conditions on surface normals not only at background pixels, but also at singular points like white pixels (where normals are equal to the light direction L). This helps to overcome the concave/convex ambiguity and to drive the resolution towards the expected result. In the rest of the paper we will denote by $\nu \in \mathbb{R}^{2M}$ the unknown vector, with $M < nm$. Discretized version of problems (3)-(5) are then easily derived using (6)-(8).

Here we change point of view and consider the following formulation of the SFS problem, alternative to (3):

$$\begin{aligned} \min \mathcal{S}(p, q) \\ \mathcal{B}(p, q) = 0, \end{aligned} \quad (9)$$

and its discretization, which does not depend on the smoothing parameter λ_S :

$$\begin{aligned} \min S(\nu) \\ b_{i,j}(\nu) = 0, \quad (i, j) \in \Omega_D, \end{aligned} \quad (10)$$

where $b_{i,j}(\nu) = E_{i,j} - \rho L^T \mathcal{N}_{i,j}(\nu_{i,j})$. Observe that the global minimizer of (9) is the smoothest surface which satisfies the brightness constraint. In the next section we will see how, by using a penalty quadratic minimization

approach [22], the solution of the constrained problem (10) can be reduced to the solution of a sequence of unconstrained minimization problems of form

$$\min_{\nu \in \mathbb{R}^{2M}} f(\nu) = B(\nu) + \lambda_S S(\nu), \quad (11)$$

which is in fact the discretization of problem (3); but thanks to the penalization approach the smoothing parameter λ_S is adaptively adjusted and does not need to be fixed in advance.

3. Regularized quadratic penalization

Quadratic penalization is a well known approach to constrained optimization [22], where constraints are embedded in the objective function by adding a suitable *quadratic penalty* term. In the case of our model problem (10), the new objective function, named quadratic penalty function, takes the form

$$Q(\nu, \mu) = S(\nu) + \mu \sum_{(i,j) \in \Omega_D} b_{i,j}^2(\nu) = S(\nu) + \mu B(\nu).$$

The scalar $\mu > 0$ is called penalization parameter; by driving it to infinity the constraints violation is penalized with increasing severity, and given a sequence of values $\{\mu_r\}_{r=1}^\infty$ such that $\mu_r \rightarrow \infty$, the solution of (10) is reduced to the following sequence of unconstrained problems:

$$\min_{\nu} Q(\nu, \mu_r), \quad r = 1, 2, \dots, \quad \text{with } \mu_r \rightarrow \infty. \quad (12)$$

This approach is theoretically motivated by the following Theorem.

Theorem 3.1. [22, Theorem 17.1]

Given a sequence $\{\mu_r\}_{r=1}^\infty$ such that $\mu_r \rightarrow \infty$ for $r \rightarrow \infty$, let $\bar{\nu}_r$ be a global minimizer of $Q(\nu, \mu_r) = S(\nu) + \mu_r B(\nu)$. Then any limit point $\bar{\nu}$ of $\{\bar{\nu}_r\}_{r=1}^\infty$ is a global solution of (10).

The next result concerns the convergence behaviour of the smoothing term. It shows that, starting from the value $S(\bar{\nu}_1)$, attained at the global minimizer of $Q(\nu, \mu_1)$, the value of the smoothing term increases through the iterations. In other words, the surface computed at each iteration r of the penalization process is driven to a surface progressively less smooth but closer to satisfy the irradiance equation.

Proposition 3.1. *Given an increasing sequence $\{\mu_r\}_{r=1}^\infty$ such that $\mu_r \rightarrow \infty$ for $r \rightarrow \infty$, let $\bar{\nu}_r$ be a global minimizer of $Q(\nu, \mu_r) = S(\nu) + \mu_r B(\nu)$. Then $S(\bar{\nu}_r) \geq S(\bar{\nu}_{r-1})$ and $B(\bar{\nu}_r) \leq B(\bar{\nu}_{r-1})$.*

Proof Using the fact that $\bar{\nu}_r$ is a global minimizer of $Q(\nu, \mu_r)$ we get

$$S(\bar{\nu}_r) + \mu_r B(\bar{\nu}_r) \leq S(\bar{\nu}_{r-1}) + \mu_r B(\bar{\nu}_{r-1}) \quad (13)$$

$$S(\bar{\nu}_{r-1}) + \mu_{r-1} B(\bar{\nu}_{r-1}) \leq S(\bar{\nu}_r) + \mu_{r-1} B(\bar{\nu}_r). \quad (14)$$

Then, dividing (13) by μ_r , (14) by μ_{r-1} , and taking sums, we have

$$\left(\frac{1}{\mu_r} - \frac{1}{\mu_{r-1}}\right)(S(\bar{\nu}_r) - S(\bar{\nu}_{r-1})) \leq 0,$$

Algorithm 3.1: Regularized Quadratic Penalty Method for SFS

Given a starting point ν_0 , $\lambda_1 > 0$, a sequence of tolerances $\{\epsilon_r\}_{r=1}^\infty \rightarrow 0$ and a positive sequence $\{c_r\}_{r=1}^\infty \rightarrow c \geq 0$

1. For $r = 1, 2, 3, \dots$
 - 1.1 Find an approximate minimizer ν_r of $Q_r(\nu, \lambda_r)$ by applying a method for unconstrained minimization problems, with ν_{r-1} as initial guess and ϵ_r as stopping criterion tolerance
 - 1.2 If a convergence test is satisfied then return the approximate solution ν_r and stop
 - 1.3 Choose a new penalty parameter $\lambda_{r+1} < \lambda_r$

that is $S(\bar{\nu}_r) \geq S(\bar{\nu}_{r-1})$ as $\mu_r > \mu_{r-1}$. Moreover, from (13) it follows

$$\mu_r(B(\bar{\nu}_r) - B(\bar{\nu}_{r-1})) \leq S(\bar{\nu}_{r-1}) - S(\bar{\nu}_r) \leq 0,$$

which yields

$$B(\bar{\nu}_r) \leq B(\bar{\nu}_{r-1}).$$

□

Note that μ_r in (12) plays the same role of $1/\lambda_S$ so that (12) is equivalent to a sequence of unconstrained problems of form (11) obtained by driving to zero the smoothing parameter.

Despite theoretical results, as shown in Section 5 we often observed good iterates going undetected as well as some iterate walking away from the sought solution with subsequent iterations unable to drive back towards it. Similar difficulties, which are typical of inverse problems, are mainly due to the fact that the sought solution may not solve (10), in particular when noise and/or discretization errors are present. Here we propose to cope with this well known problem of the variational approach to SFS by adding some regularization. In particular, we add the term $c_r \|\nu - \nu_{r-1}\|_2^2$ to the quadratic penalty function $Q(\nu, \mu_r)$, where $\{c_r\}_{r=1}^\infty$ is a sequence of positive terms converging to a value $c \geq 0$. Letting $\lambda_r = 1/\mu_r$, for each r we finally solve

$$\min_{\nu} Q_r(\nu, \lambda_r) = \frac{1}{\lambda_r} B(\nu) + S(\nu) + c_r \|\nu - \nu_{r-1}\|_2^2. \quad (15)$$

Theoretical results (i.e. Theorem 3.1 and subsequent Theorem 3.2) require to compute the global minimizer of (12) at each iteration r . In order to obtain a less expensive process it is common practice to compute a sequence of approximate minimizers, obtained by minimizing (12) with increasing accuracy for $r \rightarrow \infty$. This is justified by Theorem 17.2 in [22] for the case $c_r = 0$, $r = 1, 2, \dots$. The overall procedure, is sketched in Algorithm 3.1.

A few general comments are in order, while detailed algorithmic issues and choices are discussed in the next section. The *outer iteration* starting at Step 1 is in fact a continuation procedure on the smoothing parameter λ_S . At

each continuation step, the approximate solution ν_r can be obtained by any solver for unconstrained minimization (*inner iteration*). Note that, by driving to zero the sequence of tolerances $\{\epsilon_r\}$, the unconstrained problems (15) are solved with increasing accuracy. This allows to avoid oversolving when high accuracy is not needed, that is when λ_r is not small enough and we are still far from the sought solution. Further, the previous computed iterate ν_{r-1} is an available good initial guess for the inner iterative solver at Step 1.1. This way a very efficient overall procedure is obtained, as confirmed by the experiments shown in Section 4.

Remark 3.1. *The role of the term $c_r\|\nu - \nu_{r-1}\|_2^2$ is to avoid abrupt changes in the sequence $\{\nu_r\}_{r=1}^\infty$, as at each iteration the minimizer of (15) is penalized to go far away from the initial guess ν_{r-1} . Note that despite this is a Tikhonov regularization [9] here it plays also a different role. Tikhonov regularization is widely used in the solution of inverse problems under the assumption that the initial guess contains information on the true solution: the idea is to penalize large steps in order to remain close to it. In our context, however, at the beginning of the penalty process the initial guess does not contain any information on the sought solution and is generally far away from it. In this phase, drastic changes from one iteration to the next one must be avoided because they may cause undesired and/or unrecoverable irregularities in the reconstructed surfaces.*

Next Proposition shows that the introduction of the quadratic regularization term yields to a minimizer ν_r of (15) which is closer to ν_{r-1} than the minimizer of the unregularized function.

Proposition 3.2. *Let ν_r be a global minimizer of (15) and $\bar{\nu}_r$ be a global minimizer of the unregularized penalty function $Q(\nu, \mu_r) = S(\nu) + \mu_r B(\nu)$. Then*

$$\|\nu_r - \nu_{r-1}\|_2 \leq \|\bar{\nu}_r - \nu_{r-1}\|_2.$$

Proof The thesis follows easily, with $\mu_r = 1/\lambda_r$, from the fact that ν_r and $\bar{\nu}_r$ are global minimizers of (15) and $Q(\nu, \mu_r)$ respectively, so that

$$\begin{aligned} & \frac{1}{\lambda_r} B(\nu_r) + S(\nu_r) + c_r \|\nu_r - \nu_{r-1}\|_2^2 \\ & \leq \frac{1}{\lambda_r} B(\bar{\nu}_r) + S(\bar{\nu}_r) + c_r \|\bar{\nu}_r - \nu_{r-1}\|_2^2 \\ & \leq \frac{1}{\lambda_r} B(\nu_r) + S(\nu_r) + c_r \|\bar{\nu}_r - \nu_{r-1}\|_2^2. \end{aligned}$$

□

Finally, it can be shown that the sequence generated by the above framework is driven to a surface that satisfies the irradiance equation. The value of the corresponding smoothness term depends on c . In case $c = 0$ convergence to a solution of (10) is recovered; otherwise, the introduction of the regularization term allows to relax the request of finding the smoothest surface which satisfies the irradiance equation.

Theorem 3.2. *Given two positive sequences $\{\lambda_r\}_{r=1}^\infty$ and $\{c_r\}_{r=1}^\infty$, with $\lambda_r \rightarrow 0$ and $c_r \rightarrow c \geq 0$ for $r \rightarrow \infty$, let ν_r be a global minimizer of (15) such that $\|\nu_r\|_2 \leq M$, for some $M > 0$ and $r = 1, 2, \dots, \infty$. Then, any limit point ν^* of $\{\nu_r\}_{r=1}^\infty$ satisfies the irradiance equation and*

$$S(\bar{\nu}) \leq S(\nu^*) \leq S(\bar{\nu}) + c(\|\bar{\nu}\|_2 + M)^2, \quad (16)$$

where $\bar{\nu}$ is a global minimizer of (10). Moreover, if the sequence $\{\nu_r\}$ converges to ν^* , then

$$S(\bar{\nu}) \leq S(\nu^*) \leq S(\bar{\nu}) + c\|\bar{\nu} - \nu^*\|_2^2. \quad (17)$$

Finally, in case $c = 0$, any limit point of $\{\nu_r\}$ is a global minimizer of (10).

Proof Being ν_r and $\bar{\nu}$ minimizers respectively of (15) and (10), $Q_r(\nu_r, \lambda_r) \leq Q_r(\bar{\nu}, \lambda_r)$ and $B(\bar{\nu}) = 0$ hold, that is

$$\frac{1}{\lambda_r} B(\nu_r) + S(\nu_r) + c_r \|\nu_r - \nu_{r-1}\|_2^2 \leq S(\bar{\nu}) + c_r \|\bar{\nu} - \nu_{r-1}\|_2^2, \quad (18)$$

which recalling the nonnegativity of $B(\nu)$ implies

$$0 \leq B(\nu_r) \leq \lambda_r (S(\bar{\nu}) - S(\nu_r) + c_r \|\bar{\nu} - \nu_{r-1}\|_2^2).$$

The right hand side of this inequality goes to zero for $r \rightarrow \infty$, since the sequence $\{\nu_r\}_{r=1}^\infty$ is bounded, S is quadratic in ν , and $\lambda_r \rightarrow 0$; then for any limit point ν^* of $\{\nu_r\}_{r=1}^\infty$ it follows that $B(\nu^*) = 0$, and this implies that ν^* satisfies the irradiance equation. Moreover, left inequalities in (16) and (17) follow because $S(\bar{\nu}) \leq S(\nu)$ for any ν such that $B(\nu) = 0$.

>From (18) and the bound on $\|\nu_r\|_2$ we also have that

$$\begin{aligned} S(\nu_r) &\leq S(\bar{\nu}) + c_r \|\bar{\nu} - \nu_{r-1}\|_2^2 \\ &\leq S(\bar{\nu}) + c_r (\|\bar{\nu}\|_2 + M)^2. \end{aligned} \quad (19)$$

Then (16) holds for any limit point of $\{\nu_r\}_{r=1}^\infty$. Further, if the sequence $\{\nu_r\}_{r=1}^\infty$ converges to ν^* , taking the limit for r that goes to ∞ in (19) yields the right inequality in (17). Finally, if $c = 0$, from (16) it follows that

$$S(\nu^*) \leq S(\bar{\nu}).$$

Since $B(\nu^*) = 0$ and $\bar{\nu}$ is a global minimizer of (10), then ν^* is a global minimizer of (10), too. \square

4. Implementation issues

We give here a detailed description of the implemented procedure. At each outer iteration of Algorithm 3.1 the computation of an approximate minimizer of $Q_r(\nu, \lambda_r)$ is carried out by the Barzilai-Borwein method embedded in the nonmonotone line-search strategy given in [24]. This is a gradient type method that starting from an initial guess $\nu^{(0)}$, generates a sequence $\{\nu^{(k)}\}_{k=0}^\infty$ where

$$\nu^{(k+1)} = \nu^{(k)} - \alpha_k \nabla_\nu Q_r(\nu^{(k)}, \lambda_r).$$

In order to obtain a globally convergent procedure¹ the steplength α_k is selected by a back-tracking strategy that enforces the following nonmonotone decrease condition:

$$\|\nabla_{\nu} Q_r(\nu^{(k+1)}, \lambda_r)\|_2 \leq Q_{MAX} - \gamma \alpha_k \|\nabla_{\nu} Q_r(\nu^{(k)}, \lambda_r)\|_2^2, \quad (20)$$

where $\gamma \in (0, 1)$ and Q_{MAX} is defined as follows:

$$Q_{MAX} = \max \{Q^r(\nu^{(j)}, \lambda_r), j = \max(0, k - K), \dots, k\}$$

with $K \geq 0$. The choice of the first α -value distinguishes the Barzilai-Borwein approach among other gradient-type procedures. Letting

$$\begin{aligned} s_{k-1} &= \nu^{(k)} - \nu^{(k-1)} \\ y_{k-1} &= \nabla_{\nu} Q_r(\nu^{(k)}, \lambda_r) - \nabla_{\nu} Q_r(\nu^{(k-1)}, \lambda_r), \end{aligned}$$

for $k \geq 1$, the first α -value that is tempted in the back-tracking strategy is given by

$$\bar{\alpha}_k = \frac{\|s_{k-1}\|_2^2}{s_{k-1}^T y_{k-1}},$$

provided that $s_{k-1}^T y_{k-1} > 0$. This way, the steplength $\alpha_k = \bar{\alpha}_k$ is always taken whenever possible, i.e when it is positive and satisfies (20).

Observe that, unlike classical monotone back-tracking strategy, condition (20) does not force a decrease of the objective function at each iteration, but ensures a reduction within K iterations. The importance of adopting a nonmonotone strategy is stressed in [11, 24], where it is pointed out that Barzilai-Borwein methods which do not permit non-monotonic steps may suffer of slow convergence; we will show the benefit of the non-monotonic rule in Section 5.2. Recently it has been shown that the effectiveness of the Barzilai-Borwein approach relies on the fact that the steplength $\bar{\alpha}_k$ implicitly contains spectral information on the Hessian of the objective function. We refer to [1] for the analysis of the connection between gradient methods behaviour and spectral properties of the Hessian matrix.

In our implementation we used $\gamma = 10^{-4}$, $K = 10$, $\alpha_0 = 1$ and stopped the Barzilai-Borwein procedure (inner iterations) whenever one of the following conditions is met:

$$\begin{cases} \|\nu^{(k+1)} - \nu^{(k)}\|_2 \leq \epsilon_r \|\nu^{(k+1)}\|_2 \text{ or} \\ \|\nabla_{\nu} Q_r(\nu^{(k)}, \lambda_r)\|_2 \leq \epsilon_r \text{ or} \\ k > k_{max}. \end{cases} \quad (21)$$

Then we set ν_r equal to the last computed iterate $\nu^{(k)}$. In our runs we set $k_{max} = 1000$ and

$$\epsilon_r = \max\{10^{-2} \times \lambda_r, 10^{-4}\}.$$

Regarding the choice of the sequence $\{\lambda_r\}_{r=1}^{\infty}$, given $\lambda_1 > 0$, we adopt the following rule:

$$\lambda_{r+1} = \lambda_r / \theta \quad r = 1, 2, \dots$$

¹We say that a method is globally convergent whenever the convergence of the generated sequence does not depend on the closeness of the initial guess to the solution of the problem.

Algorithm 4.1: Implemented algorithm

Given a starting point ν_0 , $\lambda_1 > 0$, a maximum number of iterations $r_{max} > 0$ a nonnegative sequence $c_1, \dots, c_{r_{max}}$, and a stopping tolerance $toll > 0$.

1. For $r = 1, 2, 3, \dots, r_{max}$
 - 1.1 Set $\epsilon_r = \max\{10^{-2} \times \lambda_r, 10^{-4}\}$.
 - 1.2 Apply the nonmonotone Barzilai-Borwein method to problem (15) with starting guess ν_{r-1} and stopping criterion (21).
 - 1.3 Set ν_r equal to the last iterate computed at Step 1.2.
 - 1.4 If the outer stopping criterion (22) is satisfied then return the approximate solution ν_r and stop.
 - 1.5 Set $\lambda_{r+1} = \lambda_r/1.5$.
2. Failure of the procedure is declared.

where θ is set to 1.5. Typical values for λ_1 are $10^{-2}, 10^{-1}, 1$. Numerical experiments showed that these choices are not critical.

Outer iterations are stopped by checking the variation in the brightness term. In other words, letting $toll > 0$ be a given tolerance, the continuation procedure is halted whenever the following condition

$$|B(\nu_r) - B(\nu_{r-1})| \leq toll |B(\nu_r)| \quad (22)$$

is met. Failure is declared if condition (22) is not met within r_{max} outer iterations. The procedure described so far is summarized in Algorithm 4.1.

We underline that Algorithm 4.1 requires only the evaluation of the objective function $Q_r(\nu, \lambda_r)$ and its gradient. Recall that functional S is quadratic in ν , while functional B is quadratic in $\chi(\nu)$, which is nonlinear in ν (see (2)). Then $Q_r(\nu, \lambda_r)$ takes the form

$$Q_r(\nu, \lambda_r) = \frac{1}{\lambda_r} \chi(\nu)^T A_B \chi(\nu) + \nu^T A_S \nu + c_r \|\nu - \nu_{r-1}\|_2^2 + d_B^T \chi(\nu) + d_S^T \nu,$$

where $A_B \in \mathbb{R}^{3M \times 3M}$ and $A_S \in \mathbb{R}^{2M \times 2M}$ are sparse matrices, $d_B \in \mathbb{R}^{3M}$, $d_S \in \mathbb{R}^{2M}$. The structure of A_B and A_S is inherited from the structure of S and B , and they result to have only five nonzero diagonals. Then, the number of nonzero entries is at most five times the matrix dimension. Since the evaluation of Q_r and its gradient requires only two matrix-vector products, involving A_B and A_S , this task can be carried out in a very efficient way.

5. Numerical results

In this section we will present the reconstructions computed for two given shapes, starting from synthetic images of different sizes under different light conditions:

- *donut*: 75 x 75 pixels; $L = (0.3015, 0.3015, 0.9045)^T$ (oblique lighting); number of unknowns: 7112; A_B density: $2.8 \cdot 10^{-4}$; A_S density: $6.9 \cdot 10^{-4}$;
- *face*: 503 x 447 pixels; frontal lighting; number of unknowns: 233472; A_B density: $9.5 \cdot 10^{-7}$; A_S density: $2.1 \cdot 10^{-5}$;

the density of a matrix is the number of nonzero entries divided by the total number of entries. As it is known, case studies with oblique light direction give rise to more difficult problems and more expensive resolution processes than in the case of frontal light. Indeed, functional B has a simpler form when $L = [0, 0, 1]^T$. We report on test problems arising in synthetic surfaces reconstruction in order to properly evaluate obtained result and errors that have been committed during the reconstruction process. Runs have been performed with a 1.60 GHz Intel Core(TM) i5 machine, 4GB RAM, using Matlab 2013b. Results have been obtained by using Algorithm 4.1 with $c_r = 10$, for any $r \geq 1$. This choice is mainly motivated by the fact that it provides good reconstructions in the more challenging cases (e.g. with complicated shapes, or oblique light direction). Tolerance *tol* and maximum number of iterations r_{max} were set to 10^{-5} and 30, respectively. Finally, the starting vector ν_0 , needed to start the Barzilai-Borwein procedure at the first outer iteration, corresponds to the uniform normal map parallel to the light direction, hence far from the sought surface, in any of the used test. The choice of an extremely smooth initial guess is motivated by Proposition 3.1 that shows how quadratic penalization progressively reduces the smoothness term in favour of the brightness term.

The first set of experiments is focused on the first shape, a donut-like surface. We use this test problem to compare the Regularized Quadratic Penalization method (RQP) with its *unregularized* version (UQP, Unregularized Quadratic Penalization) obtained by dropping in (15) the regularization term $c_r \|\nu - \nu_{r-1}\|_2^2$, and with the classical SFS method based on the unconstrained minimization of functional (11) (UNC). In this third case, we used the Barzilai-Borwein method to solve problem (11) with stopping criteria (21), tolerance $\epsilon_r = 10^{-4}$ and $k_{max} = 1000$. We also report on numerical tests performed to show the sensitivity of our approach to the weight c_r in the regularization term, as well as to the presence of Gaussian noise in the input image.

In the second set of experiments we show the behaviour of the proposed approach in terms of computational cost and accuracy of reconstruction. Results are shown in tables where we report the initial value of the continuation parameter (λ_1), the number of performed outer iterations (\bar{r}), the last value of the continuation parameter used for the final reconstruction ($\lambda_{\bar{r}}$), the overall number of performed Barzilai-Borwein iterations (#It-BB), the overall number of Q_r -evaluations, the time in seconds needed to reconstruct the surface (time(s)), the norm of the relative error (*err*) between the normal map of the true surface and the normal map of the reconstructed surface. To be more precise, denoting by $\bar{N} = \chi(\nu_{\bar{r}})$ the computed normal map, we report the following measure of the error:

$$err = \frac{\sum_{(i,j) \in \Omega_D} \|\bar{N}_{i,j} - N_{i,j}\|_2}{M}. \quad (23)$$

Finally, for each reconstructed shape we plot the computed surface (we recovered it from the normal map by using the approach proposed in [28]), and the image of the error matrix ERR defined as follows. Let C be the matrix whose (i, j) -entry is given by $C_{i,j} = \|\bar{N}_{i,j} - N_{i,j}\|_2$, $C_m = \min_{i,j} C_{i,j}$, and $C_M = \max_{i,j} (C_{i,j} - C_m)$. Then, $ERR_{i,j} = (C_{i,j} - C_m)/C_M$. In the following we will refer to such an image as *error image*. Errors are rescaled with respect to C_m and C_M in order to obtain a grayscale digital image with $0 \leq C_{i,j} \leq 1$.

5.1. Donut

In Figure 1 we report the input image and the corresponding surface. In Figures 2-4, for each used method we plot the reconstructed surface and the corresponding error image. We set $\lambda_S = 0.1$ for the UNC method, and $\lambda_1 = 0.1$ for RQP and UQP methods. Similar results are obtained with $\lambda_S = 10^{-2}, 0.5 \cdot 10^{-2}$ and $\lambda_1 = 0.01, 1$, in either cases. As we can see from the pictures, the regularization term is crucial to obtain a good reconstruction, as both UNC and UQP methods do not properly reconstruct the hole of the donut. We underline that the value of the error err given by (23) is about $1.64 \cdot 10^{-1}$ when the RQP method is used, while it increases to $3.84 \cdot 10^{-1}$ and $3.88 \cdot 10^{-1}$ when UQP and UNC are applied, respectively. UNC is less expensive than UQP and RQP in terms of objective function evaluations, as it requires 345 Q_r -evaluations versus 517 and 675 required by RQP and UQP, respectively. This is expected as it performs only one unconstrained minimization. However, it provides an unreliable reconstruction and higher error than RQP. On the contrary, UQP is slightly more expensive than RQP, confirming that the presence of the regularization term does not affect the computational cost of the continuation process.

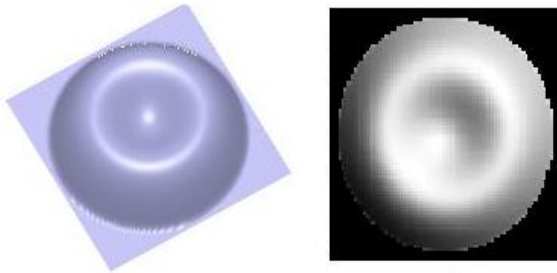


FIGURE 1. Donut: true surface (left); synthetic image (right)

More insight into the behaviour of RQP versus UQP method can be obtained using as initial guess ν_0 the vector corresponding to the normal map of the true solution. Starting with $\lambda_1 = 0.1$, in Figure 6 we show

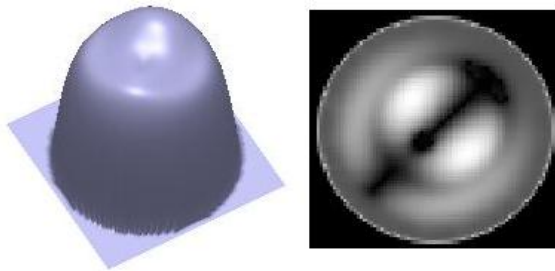


FIGURE 2. Donut, UNC method: reconstructed surface (left); error image (right)

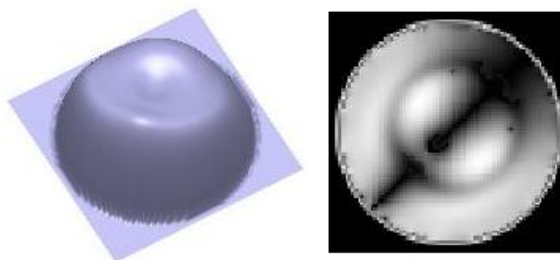


FIGURE 3. Donut, UQP method: reconstructed surface (left); error image (right)

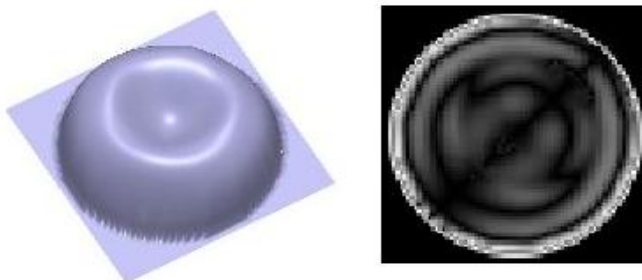


FIGURE 4. Donut, RQP method: reconstructed surface (left); error image (right)

the surface reconstructed from ν_1 , i.e. after one outer iteration of Algorithm 4.1. As we can see, the minimizer of the first unregularized functional $Q(\nu, \lambda_1) = B(\nu) + \lambda_1 S(\nu)$ is far from the initial guess. Despite the used initial guess ν_0 corresponds to the searched solution, after one iteration the method goes away from the true surface and in subsequent iterations is unable to

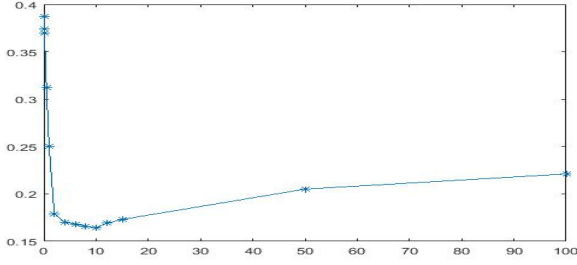
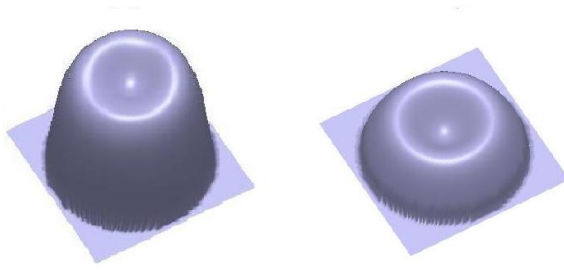
FIGURE 5. Donut, RQP method: Error versus c_r , with $\lambda_1 = 0.1$ 

FIGURE 6. Donut, reconstructions obtained starting from the normal map of the true solution, after one iteration of UQP method (left), RQP method (right)

λ_1	$\lambda_{\bar{r}}$	\bar{r}	#It-BB	#Q-eval	time(s)	<i>err</i>
0.01	$7.71e-05$	13	411	468	4.45	$2.76e-01$
0.1	$6.77e-05$	19	456	517	5.04	$1.64e-01$
1	$5.94e-05$	25	418	497	4.70	$1.54e-01$

TABLE 1. Donut: $L = [1, 1, 3]^T$, number of unknowns 7112

come back towards it. On the other hand, thanks to the presence of the term $10\|\nu - \nu_0\|_2^2$, the regularized approach remains close to the true surface.

We performed also runs by varying the weight of the regularization term. Namely, we used $c\|\nu - \nu_0\|_2^2$ with c in the interval $[0.01, 100]$. In figure 5 we plot the error *err* versus c . We can observe that large and small values of c should be avoided as we are regularizing too much or not enough. Values around 10 seem to be reliable.

In Table 1 we can observe that the overall number of Barzilai-Borwein iterations is reasonable and corresponds to the cost of solving a single unconstrained minimization problem. This behaviour is due both to the adaptive choice of the stop tolerance ϵ_r and to the good initial guesses used to initialize the Barzilai-Borwein procedure. Indeed, minimization problems are

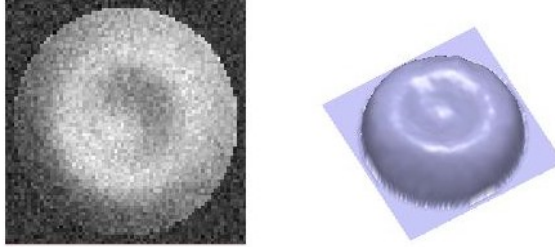


FIGURE 7. Donut: RQP method with $\lambda_1 = 0.1$, noise level 0.1: noisy image (left); reconstructed surface (right)

solved with low accuracy at the beginning of the continuation process, while accuracy requirements are increased with r . Moreover, at a generic iteration $r > 1$, the approximation ν_{r-1} computed at the previous outer iteration results to be a good approximation of the minimizer of $Q_r(\nu, \lambda_r)$. As a consequence, the average number of Barzilai-Borwein iterations performed at each outer iteration is about 30. We also observe that the overall computational time is very short, since functions and gradients can be computed at a low computational cost. As a final comment, the choice $\lambda_1 = 0.01$ seems to provide a less accurate result. This can be ascribed to the fact that this initial value is too small, and confirms the effectiveness of the continuation process to gradually drive the sequence towards the sought solution. A further evidence of the benefit of the continuation process is given by the behaviour of UNC method with $\lambda_S = \lambda_{\bar{r}}$, that is when λ_S is set equal to the final value $\lambda_{\bar{r}}$ provided by the RQP method. Indeed, starting from scratch with this λ value, UNC yields a completely inaccurate reconstruction. This is due to the fact that the continuation process provides an accurate initial guess $\nu_{\bar{r}-1}$ for minimizing $Q_{\bar{r}}(\nu, \lambda_{\bar{r}})$. On the contrary, UNC is initialized by ν_0 , which is far from the sought surface corresponding to the small smoothing parameter $\lambda_{\bar{r}}$.

In order to get an estimate of the sensitivity to noise, Gaussian noise has been added to the input image. The noisy image, with noise level 10^{-1} and the corresponding surface reconstructed by RQP are shown in Figure 7. We performed also runs varying the noise level; statistics are reported in Table 2. We note that the error err is only slightly amplified by noise (see Table 1) confirming the stability of our method with respect to noise.

We finally underline that the main difficulty in this case study lies in the oblique lighting. Indeed, the reconstruction of the Donut surface starting from a synthetic image (75 x 75 pixels in size), generated with frontal light, is

noise level	$\lambda_{\bar{r}}$	\bar{r}	#It-BB	#Q-eval	time(s)	err
0.01	$6.77e-05$	19	495	564	6.59	$1.66e-01$
0.05	$6.77e-05$	19	481	554	6.91	$1.90e-01$
0.1	$6.77e-05$	19	523	604	6.68	$2.33e-01$

TABLE 2. Donut: $L = [1, 1, 3]^T$, noisy image, RQP method with $\lambda_1 = 0.1$

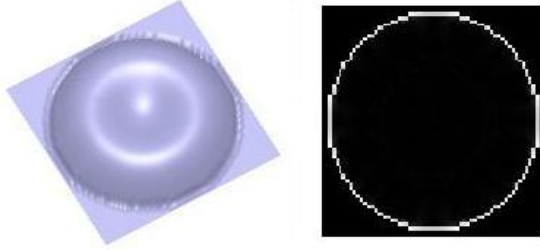


FIGURE 8. Donut with frontal light, RQP method: reconstructed surface (left); error image (right)

very accurate as it is shown in Figure 8, where $\lambda_1 = 0.1$ is used. The computed error in this case is about $5.71 \cdot 10^{-2}$, and lies entirely on the boundary of the reconstruction domain.

5.2. Face

The second treated synthetic image represents the face of a man frontally illuminated (see Figure 9). The surface is not smooth and very detailed; further this is a large test, with 233472 free variables to be determined. The results obtained with the RQP method and $\lambda_1 = 1$ are plotted in Figure 10. We can observe that, except for a small inversion of concavity/convexity in the forehead, the reconstruction is acceptable and most of the details are correctly identified. Statistics of the runs are reported in Table 3. We can observe that the number of Barzilai-Borwein iterations is still acceptable. Obviously the execution time is higher than in the Donut test due to the large dimension of the problem. All the statistics we provided so far have been obtained using the Barzilai-Borwein approach with nonmonotone decrease condition ($K = 10$ in (20)). We performed also runs with the monotonic rule ($K = 0$ in (20)) and we observed that the nonmonotonic approach allowed us to save about 10% of Barzilai-Borwein iterations and about 30% of function evaluations compared to the monotonic one.

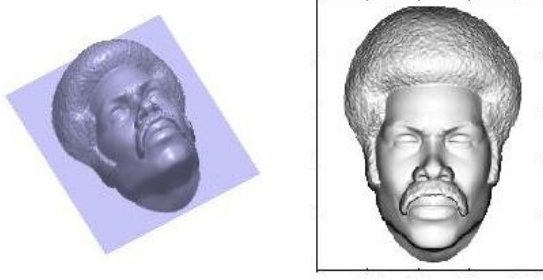


FIGURE 9. Face: true surface (left); synthetic image (right).

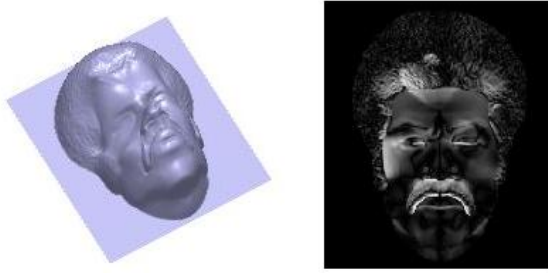


FIGURE 10. Face, RQP method: reconstructed surface (left); error image (right).

λ_1	$\lambda_{\bar{r}}$	\bar{r}	#It-BB	#Q-eval	time(s)	err
0.01	$1.16e - 04$	12	578	666	205	$1.63e - 01$
0.1	$1.01e - 04$	18	736	816	222	$1.69e - 01$
1	$8.91e - 05$	24	730	826	214	$1.68e - 01$

TABLE 3. Face: $L = [0, 0, 1]^T$, number of unknowns 233472

6. Conclusions

This work proposes a novel strategy to improve the numerical solution of the SFS problem via the variational approach. Classical methods are based on the unconstrained minimization of a suitable model, typically depending on a given smoothing parameter which markedly affects the quality of the reconstruction, and therefore the reliability of the procedure. In order to free the user from choosing a-priori the smoothing weight, here we take a different point of view and consider a constrained minimization problem. This problem is then solved by a Quadratic Penalization procedure, which in fact allows to adaptively adjust the smoothing parameter. Moreover, a quadratic regularization term is added in order to improve the robustness of the overall method.

The numerical behaviour of the proposed procedure has been tested with both frontal and oblique illuminated images. In all the reported cases, the advantage given by the use of such procedure is evident. The relative error between the original normal maps and the retrieved ones is of order 10^{-2} , and the obtained results do not depend on any problem-dependent choice of parameters. The overall computational cost, even in presence of large images, is low thanks to an efficient evaluation of objective functions and gradients.

Acknowledgements

We thank the associate editor for the care taken with this paper and the two anonymous referees for their insightful comments, which led us to improve our work. Work partially supported by INdAM-GNCS.

References

- [1] E. Birgin, J. Martínez, M. Raydan, Spectral projected gradient methods: review and perspectives, *J. Stat. Softw.* 60 (2014).
- [2] F. Camilli, M. Falcone, An approximation scheme for the maximal solutions of the Shape from Shading model. In *Proceeding of the IEEE International Conference on Image Processing*, 1 (1996), 49-52.
- [3] Y.H. Dai, R. Fletcher, Projected Barzilai-Borwein methods for large-scale box-constrained quadratic programming, *Numerische Mathematik.* 100, (2005)21–47
- [4] P. Daniel, J.-D. Durou, >From deterministic to stochastic methods for shape from shading, in: *Proceedings of the 4th Asian Conference on Computer Vision*, Taipei, Taiwan, 2000, 187–192.
- [5] R. De Asmundis, D. di Serafino, F. Riccio, G. Toraldo, On spectral properties of steepest descent methods, *IMA J. Numerical Analysis*, 33, (2013), 1416–1435
- [6] R. De Asmundis, D. di Serafino, W. Hager, G. Toraldo, H. Zhang, An efficient gradient method using the Yuan steplength, *Comput. Optim. Appl.* , 59, (2014), 541–563
- [7] J.-D. Durou, M. Falcone, M. Sagona, Numerical methods for shape-from-shading: A new survey with benchmarks, *Comput. Vision Image Understand.* 109 (2008) 22–43.
- [8] J.-D. Durou, J.-F. Aujol, F. Couteille, Integrating the normal field of a surface in the presence of discontinuities, in *Energy minimization methods in Computer Vision and Pattern Recognition* 5681 (2009) 261–273.
- [9] H.W. Engl, M. Hanke, A. Neubauer, *Regularization of inverse problems*, Kluwer Academic Publishers, 1996.
- [10] M. Falcone, M. Sagona, A. Seghini, A scheme for the Shape from Shading model with “black shadows”, *Numer. Math and Adv. Appl.* , 503-512, 2003.
- [11] R. Fletcher, On the Barzilai–Borwein method, *Optimization and Control with Applications* (L. Qi, K. Teo, X. Yang, P. M. Pardalos, D. Hearn eds), *Applied Optimization*, vol. 96. USA: Springer, pp. 235–256, 2005.

- [12] R.T. Frankot, R. Chellappa, A method for enforcing integrability in shape from shading algorithms, *IEEE Trans. Pattern Anal. Mach. Intelligence* 10 (1988) 439–451.
- [13] L. Governi, R. Furferi, L. Puggelli, Y. Volpe, Improving surface reconstruction in Shape from Shading using easy-to-set boundary conditions, *Int. J. Comput. Vision Robotics* 3 (2013) 225–247.
- [14] L. Governi, R. Furferi, M. Carfagni, L. Puggelli, Y. Volpe, Digital Bas-Relief Design: a Novel Shape From Shading-Based Method, *Comput.-Aided Design Appl.* 11 (2014) 153–164.
- [15] B.K.P. Horn, Shape from Shading: A Method for Obtaining the Shape of a Smooth Opaque Object from One View, MAC-TR-79 and AI-TR-232, Artificial Intelligence Laboratory, Massachusetts Inst. of Technology, 1970.
- [16] B.K.P. Horn, Obatinig Shape from Shading, in *The psycology of Computer visione*, Ed. P.H. Winston, McGraw Hill, 1975.
- [17] B.K.P. Horn, Height and Gradient from Shading, *Int. J. Comput. Vision* 5 (1990) 37–75.
- [18] B.K.P Horn, M.J. Brooks, The variational approach to Shape from Shading, *Comput. Vision, Graph. and Image Proc.* 33 (1986), 174–208
- [19] B.K.P Horn, M.J. Brooks, *Shape from Shading*, MIT Press Cambridge, MA, USA, 1989.
- [20] R. Kozera, Uniqueness in Shape from Shading revisited, *J. Math. Imag. Vision* 7 (1997) 123–138.
- [21] Y.G. Leclerc, A.F. Bobick, The direct computation of height from shading, in *Proceedings of the IEEE Conference on Computer Vision and Pattern Recognition*, Maui, HI, USA, 1991, 552–558.
- [22] J. Nocedal, S.J. Wright, *Numerical Optimization*, Series in operations research and financial engineering, Springer, New York, USA, 2006.
- [23] J. Oliensis, Uniqueness in Shape from Shading, *Int. J. Comput. Vision* 6 (1991) 75–104.
- [24] M. Raydan, The Barzilai and Borwein Gradient Method for the Large Scale Unconstrained Minimization Problem, *Siam J. Optim.* 7 (1997) 26–33.
- [25] E. Rouy, A. Tourin, A viscosity solution approach to Shape from Shading, *SIAM J. Numer. Anal.*, 29 (1992), 867–884
- [26] R. Szelisi, Fast Shape from Shading, *Comput. Vision, Graph. and Image Proc.: Image Understanding.* 53 (1991), 129–153
- [27] S. Tozza, M. Falcone, Analysis and approximation of some Shape-from-Shading models for non-Lambertian surfaces, *ArXiv e-prints*, eprint 1502.05197, 2016. To appear on *J. Math. Imaging Vision*.
- [28] T. Wu, J. Sun, C. Tang, H. Shum, Interactive Normal Reconstruction from a Single Image, *ACM Trans. Graph.* 27, 5, (2008) Article 119.
- [29] P. L. Worthington, E.R. Hancock, New constraints on data-closeness and needle map consistency for Shape from Shading, *IEEE Trans. on Pattern Anal. and Machine Intelligence* 21, (1999), 1250–1267.
- [30] R. Zhang, P.-S. Tsai, J.E. Cryer, M. Shah, Shape-from-shading: a survey, *IEEE Trans. Pattern Anal. Mach. Intell.* 21 (1999) 690–706.

Stefania Bellavia

S. Bellavia University of Florence, Department of Industrial Engineering, Florence I-50134, Italy

e-mail: stefania.bellavia@unifi.it

Lapo Governi

University of Florence, Department of Industrial Engineering, Florence I-50134, Italy

e-mail: lapo.governi@unifi.it

Alessandra Papini

University of Florence, Department of Industrial Engineering, Florence I-50134, Italy

e-mail: alessandra.papinii@unifi.it

Luca Puggelli

University of Florence, Department of Industrial Engineering, Florence I-50134, Italy

e-mail: luca.puggelli@unifi.it